Paleoceanography and Paleoclimatology

RESEARCH ARTICLE
10.1029/2022PA004582

The Nature of Opal Burial in the Equatorial Atlantic During the Deglaciation

I. M. Gil[1,2], J. F. McManus[3], A. Rebotim[1,2], A. Narciso[4], E. Salgueiro[1,2], and F. Abrantes[1,2]

[1]Portuguese Institute for Sea and Atmosphere (IPMA), Rua Alfredo Magalhães Ramalho 6, Algés, Portugal, [2]Center of Marine Sciences (CCMAR), Algarve University, Campus de Gambelas, Faro, Portugal, [3]Department of Earth and Environmental Sciences (DEES) and Lamont-Doherty Earth Observatory (LDEO), Columbia University, Palisades, NY, USA, [4]Madeira Interdisciplinary Centre of Marine and Environmental Research (CIIMAR-Madeira), Funchal, Portugal

Key Points:

- Microfossil evidence for the contribution by Si-rich southern-sourced water to enhanced primary productivity in the equatorial Atlantic
- The position of the intertropical convergence zone plays a role in determining the different productivity conditions
- Opal accumulation does not necessarily reflect solely diatom burial

Supporting Information:

Supporting Information may be found in the online version of this article.

Correspondence to:

I. M. Gil,
isabelle.gil@ipma.pt

Citation:

Gil, I. M., McManus, J. F., Rebotim, A., Narciso, A., Salgueiro, E., & Abrantes, F. (2023). The nature of opal burial in the equatorial Atlantic during the deglaciation. *Paleoceanography and Paleoclimatology*, *38*, e2022PA004582. https://doi.org/10.1029/2022PA004582

Received 16 NOV 2022
Accepted 30 MAY 2023

Author Contributions:

Conceptualization: I. M. Gil, J. F. McManus
Formal analysis: I. M. Gil, J. F. McManus, A. Rebotim
Funding acquisition: I. M. Gil
Investigation: I. M. Gil, A. Rebotim, A. Narciso
Project Administration: I. M. Gil
Supervision: I. M. Gil
Validation: E. Salgueiro
Writing – original draft: I. M. Gil
Writing – review & editing: J. F. McManus, A. Rebotim, A. Narciso, E. Salgueiro, F. Abrantes

Abstract Relatively high opal concentrations are measured in equatorial Atlantic sediments from the most recent deglaciation. To shed light on their causes, seven cores were analyzed for their content of siliceous (diatom, silicoflagellates, radiolarians, phytoliths, and sponge spicules) and calcareous (coccolithophores) microfossils. An early deglacial signal is detected at the time of rising boreal summer insolation ca. 18 ka by the coccolithophores. The surface freshening is likely due to the rain belt associated with the intertropical convergence zone (ITCZ), implying its southward shift relatively to its present-day average positioning. The diatom assemblages corresponding to the following increase in diatom abundances ca. 15.5 ka suggest the formation of a cold tongue of upwelled water associated with tropical instability waves propagating westward. Such conditions occur at present during boreal summer, when southerly trade winds are intensified, and the ITCZ shifts northward. The presence of the diatom *Ethmodiscus rex* (Wallich) Hendey and the coccolithophore *Florisphera profunda* indicates a deep thermocline and nutrient enrichment of the lower photic zone, revealing that Si-rich southern sourced water (SSW) likely contributed to enhanced primary productivity during this time interval. The discrepancies between the maximum opal concentrations and siliceous marine microfossils records evidence the contribution of freshwater diatoms and phytoliths, indicative of other processes. The definition of the nature of the opal record suggests successive productivity conditions associated with specific atmospheric settings determining the latitudinal ITCZ positioning and the development of oceanic processes; and major oceanic circulation changes permitting the contribution of SSW to marine productivity at this latitude.

1. Introduction

Marine productivity plays a significant role in modulating pCO_2 at present and in the past (Ahn & Brook, 2008; Siegenthaler et al., 2005), and a better understanding of the different processes and mechanisms that affect biological productivity in the ocean is crucial considering projected climate change scenarios. The productivity of diatoms (siliceous microscopic photosynthetic algae) is a major component of the biological pump leading to carbon sequestration in the deep-ocean (Abrantes & Gil, 2013; Armbrust, 2009; Nelson et al., 1995). Elevated diatom production has been hypothesized to contribute to past pCO_2 reduction during glacial times (Brzezinski et al., 2002; Matsumoto et al., 2002). The silicic acid leakage hypothesis (SALH) has been suggested as a process responsible for the observed high diatom production at low latitudes during glacial periods. This hypothesis calls for reduced silica uptake in the Southern Ocean (SO), leading to the export of Si-rich water to lower latitudes where it is utilized by diatoms, and changes in diatom productivity contributes to changes in pCO_2 on glacial interglacial timescales (e.g., Anderson et al., 2009; Arellano-Torres et al., 2011; Bradtmiller et al., 2006, 2007; Brzezinski et al., 2002; Higginson & Altabet, 2004; Pichevin et al., 2020; Romero et al., 2011). Moreover, by favoring siliceous diatom productivity over calcareous production, more carbon would be exported to the sediment (Matsumoto & Sarmiento, 2008). Evidence related to the SALH mechanism has subsequently been examined in both the Pacific and Atlantic oceans using geochemical tracers ($^{231}Pa/^{230}Th$ and opal) to calculate opal flux and burial (Bradtmiller et al., 2006, 2007). There is no consensus in support of the SALH mechanism in the glacial Equatorial Pacific Ocean (*e.g.*, Bradtmiller et al., 2006; Costa et al., 2017; Dubois et al., 2010; Thiagarajan & McManus, 2019, and references herein), however, convincing geochemical evidence was reported for the equatorial Atlantic during the last deglaciation (Bradtmiller et al., 2007). A similar increase in diatom production was also seen during the deglacial Heinrich Event 1 in the Sargasso Sea (Gil et al., 2009). One explanation provided for the SALH is a change in the nutrient concentration and transport of Southern Ocean Source

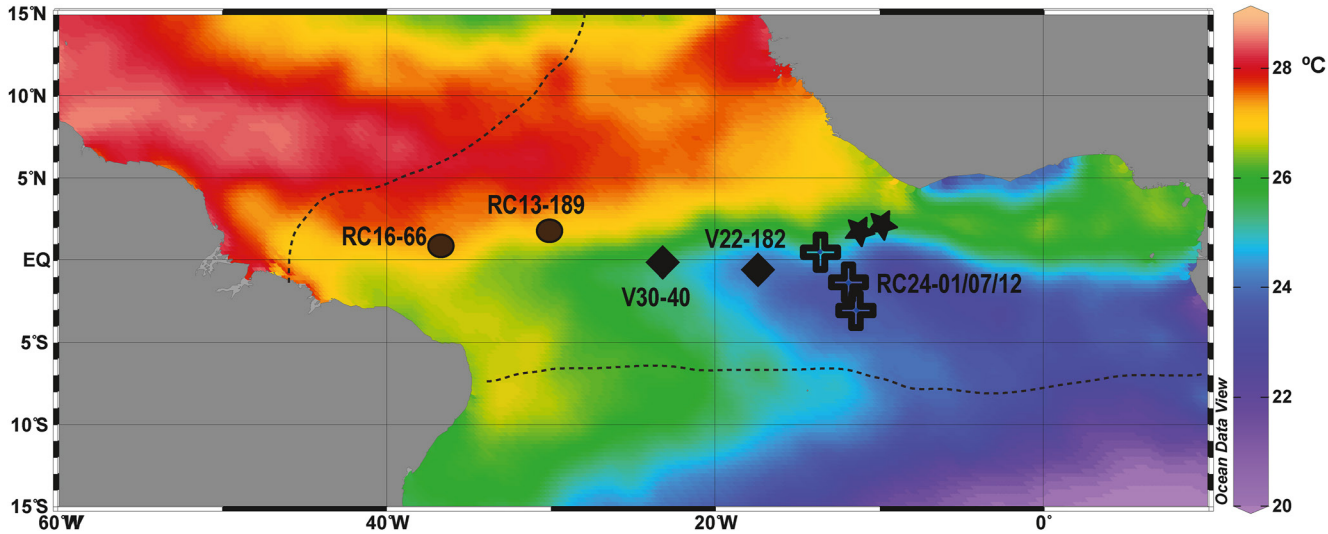

Figure 1. Location map of the studied cores. The western (RC16-66 and RC13-189), central (V30-40 and V22-182) and eastern (RC24-01, RC24-07, RC24-12) cores are represented by black dots, diamonds and crosses, respectively. Black stars represent the sediment traps commented in the text. The area where freshwater diatoms have been observed in surface sediments is delimited by dashed black lines (Schrader et al., 1993). Sea surface temperatures (July-September) are from the world ocean atlas (Locarnini et al., 2019) and evidence the area of extension the Atlantic Cold Tongue. The map was created using Ocean Data View software (Schlitzer, 2020).

Water (SSW). However, despite evidence for vigorous SO upwelling and an increase in Antarctic Intermediate Water (AAIW) northward export (Anderson et al., 2009), particularly during deglacials in the tropical Atlantic (Bradtmiller et al., 2016; Hendry et al., 2016; Poggemann et al., 2017), the possible contribution of SSW as a source of silicic acid to support diatom productivity in the Atlantic remains an open question. Specifically, it has been suggested that SSW would not be sufficiently Si-rich to explain the observed high diatom production (Meckler et al., 2013). These assessments are all based on sediment geochemical analyses of total opal accumulation, but there is currently little information available on the biological source of opal and the organisms responsible for its accumulation. Verardo and McIntyre (1994) even questioned if the sedimentary opal at this latitude is the result of surface productivity solely. Therefore, in order to determine the origin of the opal records from the equatorial Atlantic during the deglaciation and to investigate any relationship with SSW and implications for the Atlantic Meridional Overturning Circulation (AMOC), a study was undertaken to examine siliceous and calcareous micro- and nano-fossils (diatoms, radiolarians, silicoflagellates, sponge spicules, phytoliths, and coccolithophores) in conjunction with stable isotopes measurements on planktonic foraminifera in sediments deposited in the equatorial Atlantic Ocean over the last 25 ka. These data reveal important deglacial variations in the abundance and deposition of different organisms and suggest important changes in the respective local production and sedimentary contributions of each, as well as the potential for significant eolian input of opal to the marine sedimentary record.

2. Oceanographic Settings and Primary Productivity Conditions

The equatorial Atlantic surface circulation exerts a strong influence on the ocean and surrounding continents given that it controls the latitudinal position of the Intertropical Convergence Zone (ITCZ) and the related precipitation distribution (Waliser & Jiang, 2015). The study area, between 3°S and 2°N latitude (Figure 1), is influenced by both the westward Equatorial current and the Saharan atmospheric dust plume (Prospero, 1996). The position of the ITCZ controls both the wind strength and the surface-ocean currents, and consequently the latitude of the equatorial divergence (Waliser & Jiang, 2015). Although overall primary production rates are low, the area is currently characterized by two seasonal phytoplanktonic blooms associated with the seasonality of the winds. The first productivity peak occurs during the boreal summer (July to September) in response to the strengthening of the equatorial winds associated with a northward shift of the ITCZ (Pérez et al., 2005), while the second bloom, more modest, occurs in late fall-early winter in response to the relaxation of the northwest African monsoon (Grodsky et al., 2008).

During winter, more dust is emitted from the North African continent and transported southwest toward the equatorial latitude by northeasterly winds (Tegen et al., 2006; Washington et al., 2003). Those winds can also

Table 1
Cores Coordinates and Water Depth of Core Collection: RC16-66 and RC13-189 (West); V30-40 and V22-182 (Central); and RC24-01, RC24-07, and RC24-12 (East)

Core	Latitude	Longitude	Depth (m)
RC16-66	0.75	−36.617	4,424
RC13-189	1.87	−30	3,233
V30-40	−0.2	−23.15	3,706
V22-182	−0.53	−17.27	3,614
RC24-01	0.55	−13.65	3,837
RC24-07	−1.333	−11.917	3,899
RC24-12	−3.01	−11.417	3,486

transport freshwater diatoms and phytoliths from the continent to the ocean (Folger et al., 1967; Kolbe, 1957; Maynard, 1976; Pokras & Mix, 1985; Pokras & Ruddiman, 1989). Indeed, the spatial distribution of freshwater diatoms in core-top sediments corresponds to the same area that is under the influence of atmospheric dust plumes from North West Africa between 20°N and 5°S (Maynard, 1976; Pokras, 1991; Schrader et al., 1993). Variations in these inputs in the past are considered to reflect the degree of African aridity during glacial times (Parmenter & Folger, 1974). These observations are also consistent with the finding in sediment traps of freshwater diatoms in the upper 100 m of the water column and the suggestion that the winter dust plume extends as far as 25°W along the equator (Lange et al., 1994). The diatom genus *Chaetoceros* Ehrenberg (vegetative cells of neritic taxa and resting spores) indicates the southward extension of the coastal water influence in the western equatorial Atlantic (Lange et al., 1994), and could be considered allochthonous. In general, this genus is also characteristic of upwelled waters (Pitcher, 1990 and reference herein).

In summary, siliceous microfossils deposited in equatorial Atlantic sediments can originate from distinct sources: local siliceous productivity (revealed by marine diatoms, silicoflagellates, and radiolarians), external eolian input (freshwater diatoms and phytoliths) and coastal influence/upwelling (diatoms such as *Chaetoceros* resting spores). The variations in the relative abundance of these microfossils over time can therefore shed light on changes in hydrographic, atmospheric and climatic processes operating in this region.

3. Materials and Methods

3.1. Material

Sediments from seven cores collected along an east-west transect close to the Equator in the Atlantic were analyzed (Figure 1 and Table 1). The cores used and sampling are identical to those previously used by Bradtmiller et al. (2007) for geochemical analyses. Opal, $CaCO_3$ and $^{231}Pa/^{230}Th$ records are from Bradtmiller et al. (2007) as well. The detrital fraction contribution is calculated here by retrieving the opal and $CaCO_3$ contribution (in percent) from Bradtmiller et al. (2007). In total, 86 sediment samples were treated and analyzed for their siliceous microfossil and coccolithophore content.

3.2. Chronology

We used age models published by Verardo and McIntyre (1994) for cores RC16-66, RC24-01, RC24-07, and RC24-12, and age models from CLIMAP (1976) and Mix and Ruddiman (1985) for the remaining cores. They are the same used by Bradtmiller et al. (2007). The chronologies were based on benthic $\delta^{18}O$ and ^{14}C AMS ages.

3.3. Siliceous Microfossils Analyses

Siliceous microfossils were extracted from ∼1 g of dry sediment, after removal of calcium carbonate using dilute HCl and organic matter oxidation using H_2O_2 (Abrantes et al., 2005). An aliquot of the preparation was poured on a specific evaporation tray (Batterbee, 1973) containing the coverslips to be mounted. No pipette was used to avoid a size selection of the microfossils. Siliceous micro-fossils were identified and counted at 1000× magnification, using established counting protocols (Schrader & Gersonde, 1978). Three slides were counted for each sample (*cf.* Figures S1–S3 in Supporting Information S1) and the median value was used for the abundance calculation (number of diatom valves per gram). The freshwater species, *Chaetoceros* resting spores and fragments of *Ethmodiscus rex* (Wallich) Hendey were counted separately, as were radiolarians, silicoflagellates, phytoliths and sponge spicules. Diatom assemblages (Figure 4) corresponding to the opal maximum previously reported (Bradtmiller et al., 2007) and/or the maximum in diatom abundance (this work) were determined in all cores with the exception of RC16-66, which had extremely low abundances. For the diatom assemblage reconstruction, 300 specimens (not including *Chaetoceros* resting spores which were counted apart) were counted and identified for each sample. Only species with a contribution higher than 2% throughout the cores are presented since this cutoff value defines rare species (Imbrie & Kipp, 1971).

3.4. Coccolithophore Analyses

Slides for coccolithophore counts were prepared using the technique of Flores and Sierro (1997), which allows the estimation of absolute abundances (number of coccolithophore plates per gram). Coccolithophore analyses were made at 1250× magnification using a polarized-light microscope. For quantitative analysis, in random fields of view, at least 400 small coccoliths were counted, together with an independent counting of larger coccolithophore (>3.5 μm). Due to the high abundance of *Florisphaera profunda*, its nannoliths were combined with the group of the smaller *Noelaerhabdaceae* to maximize the representation of the minor components present in the assemblage. As few species constitute most of the coccolithophore assemblage, and we only present the species with a higher than 2% contribution throughout the core in all cores (*F. profunda*, *E. huxleyi*, *G. oceanica*). This is consistent with previous studies that similarly used 2% as the cutoff value to define rare species (Imbrie & Kipp, 1971).

3.5. Stable Isotopes Measurements on Planktonic Foraminifera Shells

To retrieve the foraminifera shells from the bulk sediments, the samples were weighted and washed with de-ionized water through a 63 μm mesh sieve. Stable carbon and oxygen isotopes were measured on the planktonic foraminifera *Neogloboquadrina dutertrei*, a species present throughout all intervals in all cores. The measurements were performed at the MARUM - University of Bremen (Germany). Approximately 50 μg of crashed tests were treated with 100% phosphoric acid in a Kiel-carbonate device and loaded into a Finnigan MAT 251 mass spectrometer. The precision of the measurement is ±0.07‰ and of ±0.02‰ for oxygen and carbon, respectively and the long-term reproducibility is of the analyses is ±0.08‰. Temperatures were calculated using the equation of Shackleton (1974) based on the $\delta^{18}O$ measured on the planktonic foraminifera *N. dutertrei* and the present day sea surface temperature at each site was taken from the 2009 NOAA World Ocean Atlas (Levitus et al., 2002).

4. Results

The results are presented by individual proxy to disentangle common simultaneous variations of the proxies at the different sites (Figure 2) and by regions (West, Central and East) in order to allow a direct comparison of the different proxies in each sample (Figure 3).

4.1. Similarities and Discrepancies Among the Seven Cores

All records represent at least the last 25 ka (Figures 2 and 3). Sea sub-surface temperatures (SSST) at each site were calculated from $\delta^{18}O$ of *N. dutertrei* (Figures 2a and 3a). This foraminifera is considered a thermocline-dwelling species that calcifies at the base of the upper thermocline, around 100 m depth (Farmer et al., 2007; Steph et al., 2009), with a confidence interval of 64–169 m depth (Farmer et al., 2007). With a living depth below the mixed layer, surface salinity changes due to heavy precipitations associated with the ITCZ are no expected to affect the SSST reconstruction. Importantly, this calcification depth is constant and independent of oceanographic conditions (Cléroux et al., 2013). Despite the differences in sedimentation rates of the sites and hence the age resolution of the different records, a clear increase in SSST is seen in all sites ca. 16.5 ka, except at RC13-189.

The detrital fractions and opal (Figures 3e and 3g) evolve in concert in all cores, except for site RC24-12. The opal fractions (Figures 2g and 3g) are generally low (3%–4%), but RC24-01 and RC24-07 (eastern cores) have higher opal percent (8%–11%, respectively). All cores contain diatoms (Figures 2h and 3h). High diatom abundances are centered at ca. 15.5 ka (except in RC16-66 where diatoms start to appear at 15.5 ka and the maximum is centered ca. 5 ka). The highest diatom abundances correspond to the maxima in opal and $^{231}Pa/^{230}Th$ (Figures 3h, 3g, and 3f) in the eastern cores (RC24-01, RC24-07 and RC24-12). In RC24-07, this also corresponds to maxima in *Chaetoceros* resting spores and freshwater diatoms (Figures 3j and 3k). In V22-182, the highest opal contents recorded corresponds to maximum abundance of freshwater diatoms (Figures 3g and 3k) and in V30-40, the diatom and others siliceous microfossils maxima are centered ca. 16 ka and precede the opal maxima by about 1 ka (Figures 3g, 3h, and 3m).

Diatom assemblages are presented in Figure 4. *Thalassionema nitzschioides* (Grunow) Mereschkowsky is the most abundant diatom (>15%) in all cores during the period of maximum diatom abundance and/or high opal content, except in RC24-12 where it is *Thalassiosira oestrupii* (Ostenfeld) Proschkina-Lavrenko ex Hasle. This last species is however the second most abundant diatom in the remaining eastern cores (RC24-01 and RC24-07), while *T. nitzschioides* is the second most abundant in RC24-12. *Nitzschia interruptestriata* Simonsen is the second most abundant in the western core (RC13-189); and *Nitzschia bicapitata* Cleve and *Rhizosolenia*

10.1029/2022PA004582

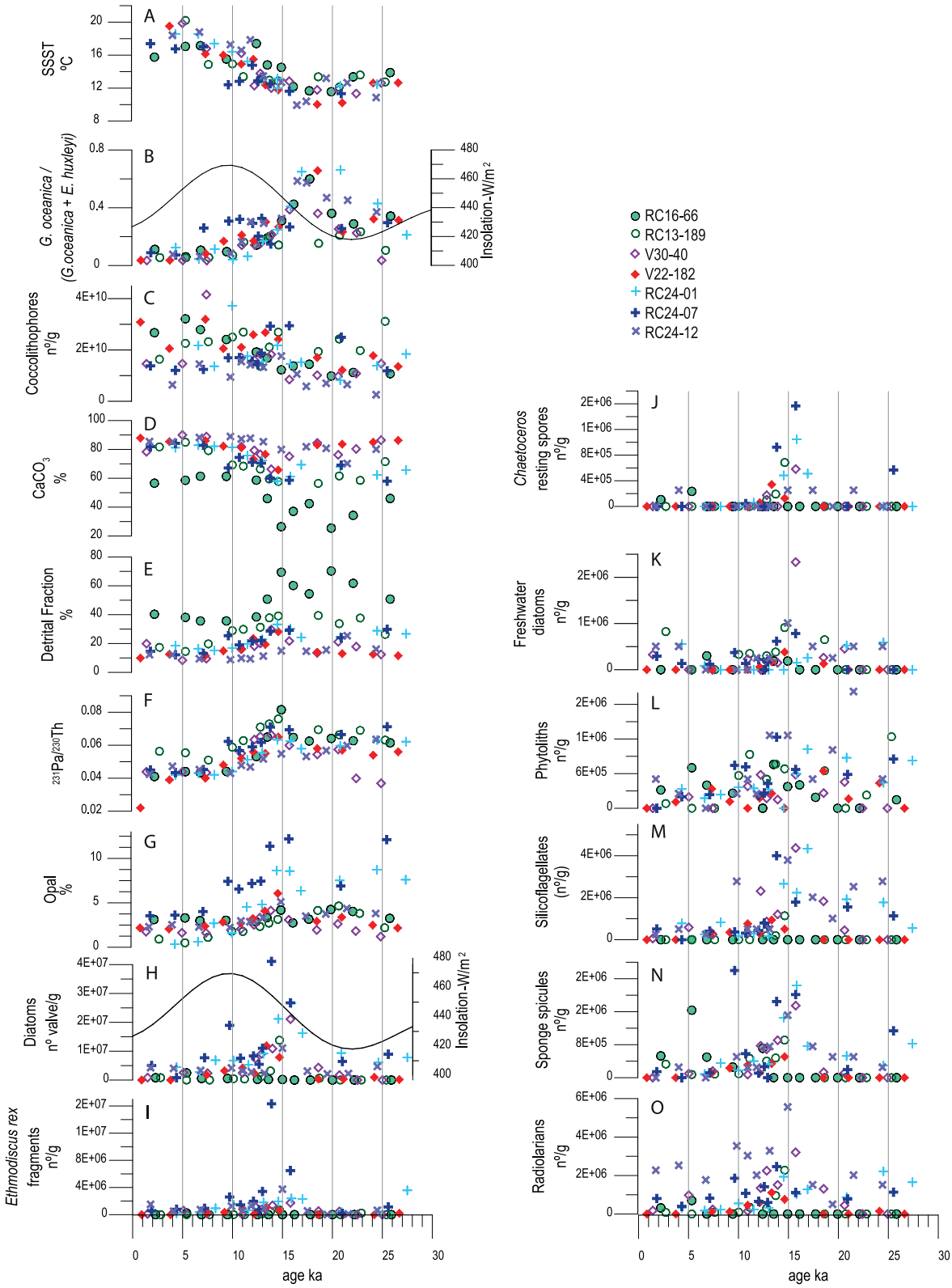

Figure 2.

bergonii Peragallo are the secondly most abundant species in the central cores (V30-40 and V22-182). In the western cores, the third most abundant (>10%) species are *R. bergonii*, *Fragilariopsis doliolus* (Wallich) Medlin & Sims, *Chaetoceros* resting spores and *Azpeitia nodulifera* (Schmidt) Fryxell & Sims. The most common freshwater diatom species found are principally centric forms that belong to the genera *Aulacoseira* (such *A. ambigua* (Grunow) Simonsen, *A. granulata* (Ehrenberg) Simonsen) and *Stephanodiscus* (*S. hantzschii* Grunow in Cleve and Grunow and *S. minutulus* (Kützing) Round), as in previous studies.

In the western cores, the peaks in opal and/or $^{231}Pa/^{230}Th$ (Figures 3f and 3g) do not only correspond to increased total marine diatom abundance (Figure 3h): in RC16-66, high opal values correspond to high abundances of freshwater diatoms and phytoliths (Figures 3g, 3k, and 3l) and the high opal content at 20 ka is not associated with any siliceous microfossil counterpart (Figures 3g and 3m). In RC13-189, the diatom maximum recorded ca. 15 ka is not detected in the opal record (Figures 3h and 3g).

The absolute abundance of coccolithophores fluctuates around 3×10^{10} coccolithophore plates per gram (Figure 2c), except in RC24-12 where they are much less abundant. The highest abundance is observed in RC24-01, at 10 ka (Figure 3d), and in V30-40, ca. 7.5 ka (Figure 3d). In the western cores, the peaks in total coccoliths (RC16-66, ca. 5.5 ka; RC13-189, ca. 15 ka) coincide with the highest abundances of most other proxies. *F. profunda* is the dominant species (Figure 3c), with relative abundances between 40% and 81% per sample, followed by *E. huxleyi* (10%–28%) and *G. oceanica* (1%–24%). In general, when the abundance of *F. profunda* increases, *G. oceanica* (Figure 3b) decreases particularly in cores RC16–66, V22-182, RC24-01, RC24-07, and RC24-12 (with the correlation coefficients of −0.89, −0.82, −0.87, −0.59 and −0.73, respectively). The contribution of *G. oceanica* is higher than the contribution of *E. huxleyi* (Figure 3b) between 15.8 and 23 ka in cores RC16-66 (17.8 ka), V22-182 (18.6 ka), RC24-01 (15.9–23 ka), RC24-12 (16.5–19 ka). There are no data-points corresponding to this interval in RC13-189 and RC24-07. The relationship between these two species is made evident by the ratio *G. oceanica*/(*G. oceanica* + *E. huxleyi*) in Figure 2b.

4.2. Differences Among Equatorial Atlantic Regions

4.2.1. The Western Equatorial Atlantic: RC16-66 and RC13-189

RC16-66 presents SSST changes of larger amplitude than RC13-189 (Figure 3a). After a marked increase starting ca. 16 ka, culminating ca. 12.5 ka (+5°C), the SSST shows little variation (except a brief diminution of −∼1.5°C at ca. 9.5 ka). The RC13-189 SSST record is roughly constant until an abrupt increase in temperatures ca. 11 ka.

By 15 ka, all siliceous microfossils are notably more abundant in RC13-189 (Figures 3h–3m), while only freshwater diatoms and phytoliths are more abundant in RC16-66 (Figures 3k and 3l). Diatoms were almost absent from RC16-66 sediments until ca. 15.5 ka (Figure 3h) and their abundance increased only afterward. Both coccoliths and diatoms reached their highest abundance much later (Figures 3d and 3h), at ca. 5.5 ka, along with *Chaetoceros* resting spores and *Ethmodiscus rex* fragments, radiolarians and sponge spicules (Figures 3i, 3j, and 3m). Freshwater diatoms and phytoliths abundances varied in concert and were more abundant during two periods (Figures 3k and 3l): at ca. 20-12.5 ka in both cores (when the contribution of the detrital fraction of the sediment were also more important) and at ca. 9.2-2 ka in RC16-66 only.

$CaCO_3$ was the dominant component in RC13-189 (Figure 3e) and increased from ca 14 ka to the present in both cores.

4.2.2. The Central Equatorial Atlantic: V30-40 and V22-182

The most notable increase in SSST started at ca. 12 ka in V30-40 and at ca. 13.5 ka in V22-182 (Figure 3a). In V30-40, the maxima in siliceous microfossils (ca. 16 ka) occurred before the maxima in $^{231}Pa/^{230}Th$ and opal

Figure 2. RC16-66 (black rounded green dot), RC13-189 (green circle), V30-40 (purple diamond), V22-182 (plain red diamond), RC24-01 (light blue cross), RC24-07 (bold dark blue cross) and RC24-12 (purple cross) records presented altogether by proxy: (a) Sea sub-surface temperature in degrees Celsius (°C) calculated with the equation of Shackleton (1974) using the $\delta^{18}O$ measured on the planktonic foraminifera *N. dutertrei* and the present day SST over the site obtained from the NOAA database (Levitus et al., 2002); (b) ratio between *G. oceanica* and *E. huxleyi* (% (*G.oceanica*/(% *G. oceanica* + % *E. huxleyi*)) indicative of surface water freshening versus solar insolation in June at 60° North (Berger, 1992); (c) Coccolithophore plates abundances in number per gram (n°/g); (d) Calcium carbonate—$CaCO_3$ in percent from Bradtmiller et al. (2007); (e) Detrital fraction in percent from Bradtmiller et al. (2007); F- $^{231}Pa/^{230}Th$ ratio from Bradtmiller et al. (2007); (f) Opal in percent from Bradtmiller et al. (2007); (h) Diatom abundance in number of valves per gram (n°/g) versus solar insolation in June at 60° North (Berger, 1992); (i) *Ethmodiscus rex* fragments in number per gram (n°/g); (j) *Chaetoceros* resting spores in number per gram (n°/g); (k) Freshwater diatoms in number of valves per gram (n°/g); (l) Phytoliths in number per gram (n°/g); (m) Silicoflagellates in number per gram (n°/g); (n) Sponge spicules in number per gram (n°/g); (o) Radiolarians in number per gram (n°/g).

10.1029/2022PA004582

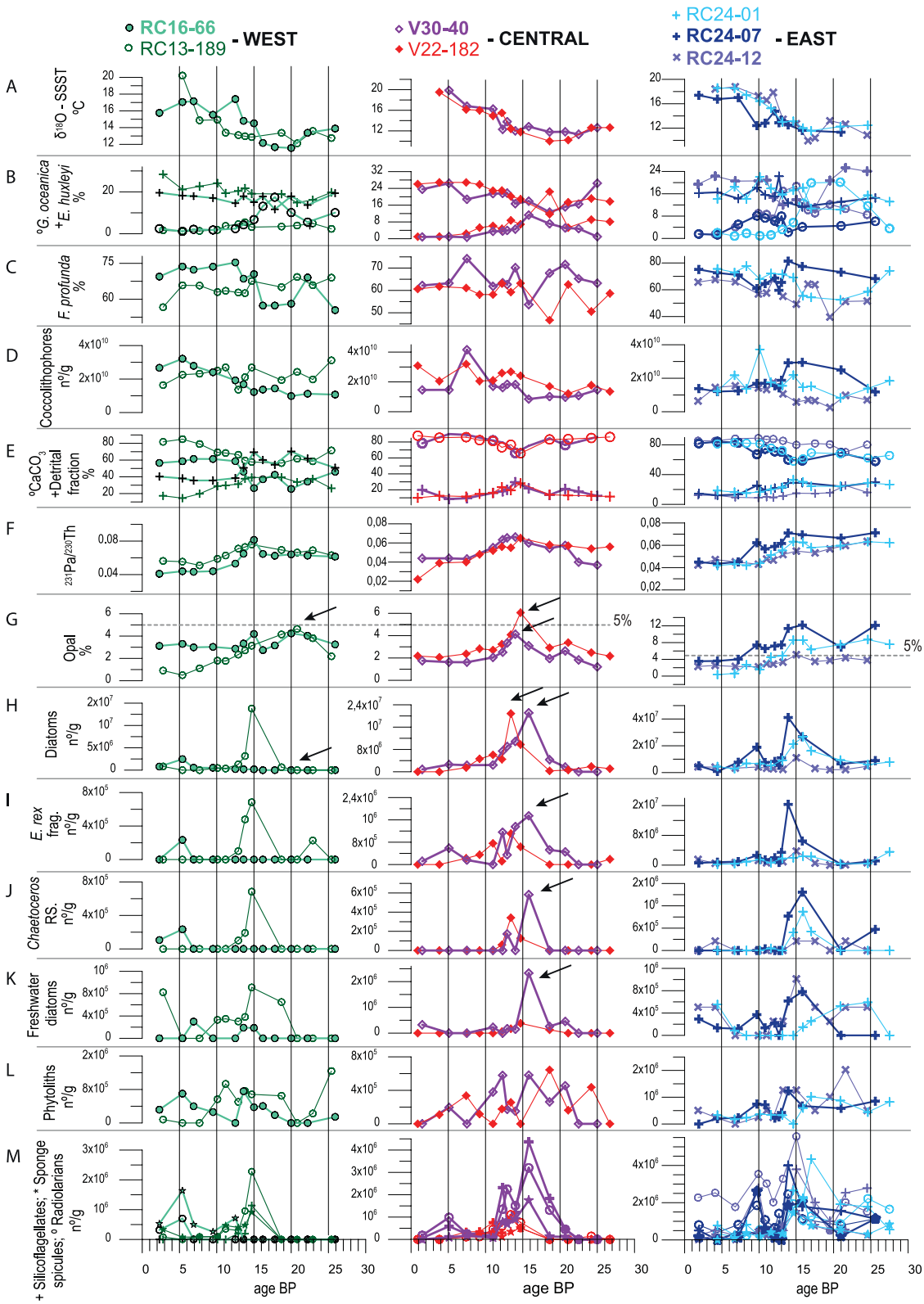

Figure 3.

10.1029/2022PA004582

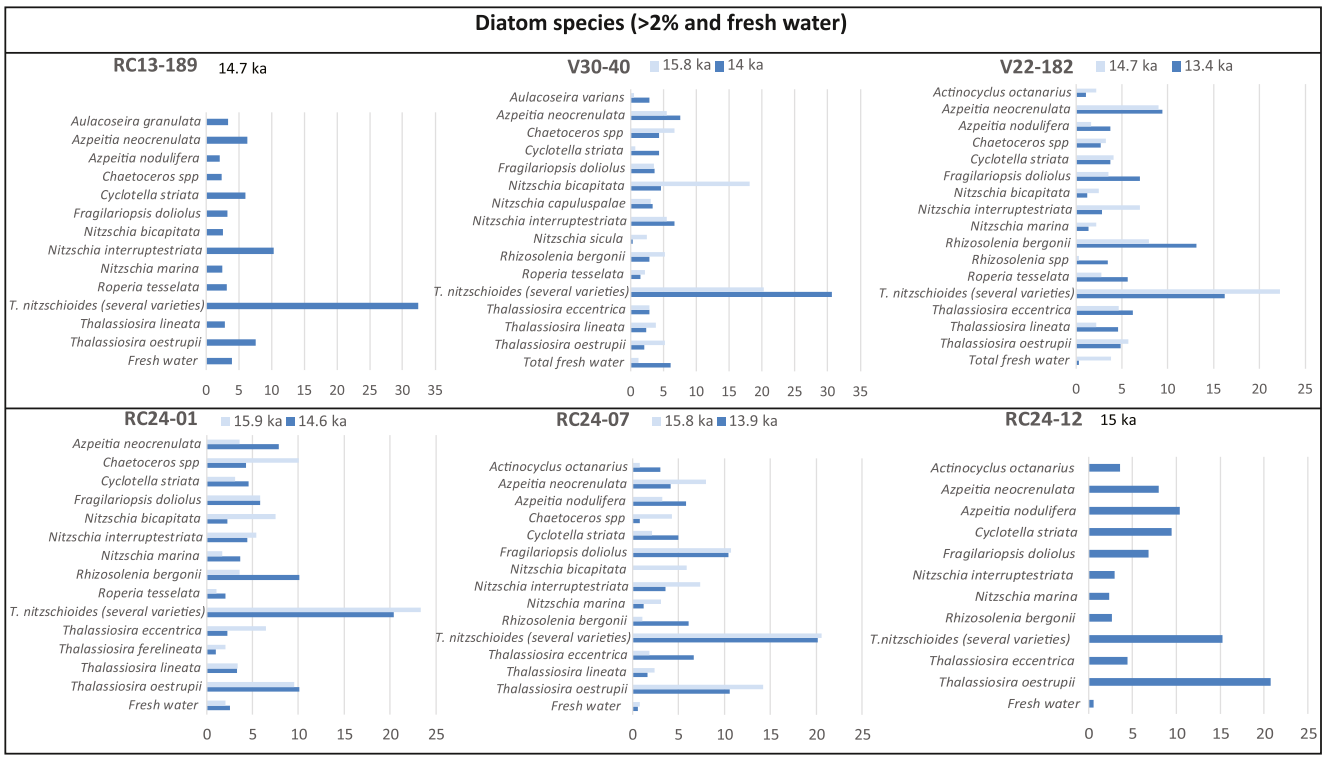

Figure 4. Diatom assemblages for the time intervals of maximum diatom abundance for cores RC13-189 (at 14.7ka), V30-40 (at 15.8 and 14 ka), V22-182 (at 14.7 and 13.4 ka), RC24-01 (15.9 and 14.6 ka), RC24-07 (15.8 and 13.9 ka), and RC24-12 (15 ka). Species presented include all diatom species contributing >2% of the total as well as freshwater diatoms.

(Figures 3f and 3g), while in V22-182 it occurred after the maxima in opal and $^{231}Pa/^{230}Th$ at ca. 14.5 ka (except for the abundance of freshwater diatoms which is coincident). The $CaCO_3$ fraction was the most dominant fraction in sediments of both cores (Figure 3e). Phytoliths were more abundant at ca. 24, 17.5, 13.5, 7.5 ka in V22-182 and 21, 16 and 12 ka in V30-40 (Figure 3l). The coccolithophore abundance was elevated after ca. 14 ka in V22-182, with a maximum ca.7.5 ka in both cores (Figure 3d). The assemblages are dominated by *F. profunda* (Figure 3c), with maximum scores ca. 7.5 ka in both cores. The maximum contribution of *G. oceanica* at ca. 16 ka occurred at the same time as the diatom and *Chaetoceros* resting spores maximum abundance in V30-40 (Figures 3b and 3j).

4.2.3. The Eastern Equatorial Atlantic: RC24-01, RC24-07, and RC24-12

In this area, the cores are distributed over a range of latitudes resulting in SSST differences (Figure 3a). At site RC24-01, north of the equator the SSST are steady until ca. 16 ka when they started to increase regularly, with a modest pause ca. 13 ka. In the core just south of the equator (RC24-07), SSST reach the maximum at ca. 12 ka following a slow rise of ~3°C initiated at ca. 15 ka. This is followed by a marked decrease (- ~2°C) ca. 9.5 ka, after which the SSST rose by +~4.5°C until ca. 7 ka and remain stable after. The SSST in the core furthest south (RC24-012) started rising ca. 16.5 ka achieving a maximum at ca. 12 ka (+8°C).

The highest opal (Figure 3g) content in all three eastern equatorial cores appears to be coincident with high siliceous production (Figures 3i, 3j, 3k, and 3m) which consists of diatoms (including *Chaetoceros* resting spores, *E.*

Figure 3. Microfossils, isotopic and geochemical records from the Western cores (RC16-66 (black rounded green dot, bold line) and RC13-189 (green circles), left panel; Central cores (V30-40—open purple diamond, bold line and V22-182—red diamond), central panel; and Eastern cores (RC24-01—light blue cross, RC14-07—bold dark blue cross, bold line and RC24-12—purple cross), right panel: (a) Sea sub-surface temperature in degrees Celsius (°C) calculated with the equation of Shackleton (1974) using the $\delta^{18}O$ measured on the planktonic foraminifera *N. dutertrei* and the present day SST over the site obtained from the NOAA database (Levitus et al., 2002); (b) Abundance in percent of the coccolithophores *G. oceanica* (circle) and *E. huxleyi* (cross); (c) Abundance in percent of the coccolithophore *F. profunda*; (d) Abundance of the coccolithophore plates in number per gram (n°/g); (e) Percentages of calcium carbonate (circle, $CaCO_3$) and detrital fraction (cross) from Bradtmiller et al. (2007); (f) $^{231}Pa/^{230}Th$ ratio from Bradtmiller et al. (2007); (g) Opal in percent from Bradtmiller et al. (2007); (h) Diatom abundance in number of valves per gram (n°/g); (i) Abundance of *Ethmodiscus rex* fragments per gram (n°/g); (j) *Chaetoceros* resting spores abundance in number of valve per gram (n°/g); (k) Freshwater diatom abundances in number per gram (n°/g); (l) Abundance of phytoliths in number per gram (n°/g); (m) Abundance of silicoflagellates (cross), sponge spicules (star) and radiolarians (circle) in number per gram (n°/g).

rex fragments) and other siliceous microfossils (ca. 18–14 ka in RC24-01; 16–14 ka in RC24-07 and ca. 16.5-14 ka in RC24-12).

Freshwater diatoms and phytoliths were abundantly present between ca. 24-17 ka in RC24-01 and decreased thereafter (Figures 3k and 3l). In RC24-12, phytoliths show a maximum at ca. 22 ka and decrease from there to the present, although this decrease is punctuated with relatively higher values between 15 and 13 ka (Figure 3l). In RC24-07, the highest values of opal (11%) are at ca. 15.7 ka, and it corresponded to an increase in *Chaetoceros* resting spores and freshwater diatoms (Figures 3g, 3j, and 3k). This is followed by a diatom (including *E. rex*) and phytoliths maxima by 14 ka (Figures 3h, 3i, and 3l).

$CaCO_3$ is the highest fraction in all cores (Figure 3m), but the presence of coccolithophores differs among cores and with time. Their abundance is outstandingly high ca. 10 ka in RC24-01 (dominated by *E. huxleyi)*, while their abundance is low in RC24-07 particularly since 14 ka. In RC24-12, there are three maxima at ca. 7, 11, and 15 ka. The relatively lower contributions of *F. profunda* (Figure 3c) between ca. 25 and 16 ka in RC24-01 corresponded to the highest contributions of *G. oceanica* (Figure 3b), which registered extremely low values after ca. 12 ka. The contribution of *G. oceanica* was also high ca. 16.5 ka in RC24-12, but not in RC24-07.

5. Discussion

5.1. Geochemical and Microfossil Records Comparison

All cores, with the exception of core RC13-189 (Figure 3a), show a distinct SSST increase at ca. 16.5 ka indicative of the deglaciation onset in this area (Figure 2a).

Bradtmiller et al. (2014) suggested that core RC13-189 and RC-16-66 deglacial samples may represent a level of intense scavenging possibly due to either sediment runoff from the Amazon basin, mass wasting events or nepheloid-transported. All these processes can affect the sedimentary record and might explain the absence of increased SSST in RC13-189, although RC16-66 samples do record the SSST increase indicative of the deglaciation. RC16-66, however, differs from the other sites, as it records a maximum diatom abundance at ca. 5 ka and not ca. 15.5 ka. Phytoliths and freshwater diatoms are abundant during this older time of the deglaciation, pointing to intensified winds from the African continent to the ocean. Indeed, the African dust can reach as far as the Caribbean (Prospero et al., 1970). Again, the difference between RC16-66 and the other sites could be due to its westernmost position and the possible influence of the South American continent.

In general, the siliceous microfossil record and the opal data at many of the cores are not comparable, with opal maxima not corresponding to an increased abundance of siliceous microfossils, and/or the maxima in opal not corresponding to the maximum in total diatom abundance (arrows in Figure 3). In fact, these opal maxima seem to correspond specifically to the high abundance of one diatom group, such as the *Chaetoceros* resting spores, freshwater diatoms or another siliceous microfossil (as the phytoliths). It is particularly clear in the western cores (arrows in Figures 3g–3k). In RC16-66, the highest opal values ca. 20 ka do not correspond to a peak in the abundance of any siliceous microfossil, while ca. 15 ka it corresponds to freshwater diatoms and phytoliths. In RC13-189, the opal maximum ca. 21 ka does not correspond to any siliceous microfossil, while the maximum in all siliceous microfossils (including diatoms) ca. 15 ka is not reflected by the opal record (Figures 3h–3m). In the central cores (arrows in Figures 3g–3k), the maximum in opal ca. 14 ka in V30-40 does not correspond to the maximum abundance of siliceous microfossils, which occurs in general ca. 16 ka. In the same core, relatively more elevated opal values ca. 21 ka correspond to increased abundance of phytoliths, freshwater diatoms and *E. rex* fragments. In V22-182, again, the maximum in opal ca. 15 ka does not correspond to the maxima in siliceous microfossils, which in this case occur later, ca. 13.5 ka. Finally, in the eastern cores (Figure 3g), although the opal records display limited variability, the main maximum in opal ca. 15 ka corresponds to an increase in siliceous microfossils. However, in RC24-12, it better reflects an increase in freshwater diatoms, phytoliths or other microfossils (Figures 3k, 3l, and 3m) than diatom production (Figure 3h), while in RC24-01 and RC24-07, it reflects indeed diatom production.

The deviation between the opal record and marine diatom abundance could be due to the method used for opal analysis. Indeed, Mortlock and Froelich (1989) compared several leaching methods and suggested that opal values below 5% (such as in cores RC16-66, RC13–189, V30-40, and RC24-12), particularly in samples with high clay content, should be interpreted with caution. Moreover, we note that different siliceous microfossils are

of different size and density and some microfossils contain more opal than others. For example, in our cores, most of the marine diatoms species that are responsible for ocean productivity are less robust than any of the other siliceous microfossils identified (*i.e.*, radiolarians, sponge spicules, and phytoliths), which are already recognized as an important sink for silicon (Maldonado et al., 2019). Even within the diatoms, freshwater diatom species contain more opal than marine species (Conley et al., 1989). Therefore, bulk analysis of opal to evaluate the marine diatom productivity must also be regarded with caution if these other siliceous microfossils are present. This is particularly important in the zone of our study, which receives considerable amounts of African dust that can contain phytoliths and freshwater diatoms blown from the continent. Local diatom production could be substantially more elevated at a time, but it may not always correspond to increased opal and/or lower $^{231}Pa/^{230}Th$ ratios. We conclude that the distribution of diatom species (*Chaetoceros* resting spores, freshwater species) and abundance of other microfossils in these records indicates that processes other than local diatom production, such as eolian and coastal influence, contributed to the observed opal maxima. Our records sustain therefore the earlier hypothesis formulated by Verardo and McIntyre (1994) based on a similar set of cores that the sedimentary opal at this latitude is not only the result of surface productivity.

5.2. Diatom Productivity Conditions During the Deglaciation

The diatom assemblages during the periods of maximum diatom abundance (Figures 3h and 4) indicate more precisely the characteristics of the overlying surface water. To assist the interpretation of these diatom assemblages, and confirm if the microfossil assemblages in sediment reflect the assemblages present in the overlying water column, many studies of surface sediments (Pokras, 1991; Pokras & Mix, 1985; Pokras & Molfino, 1986; Van Iperen et al., 1987) and sediment traps (Lange et al., 1994; Treppke et al., 1996) from the equatorial Atlantic, and in particular from its eastern part (the Gulf of Guinea), are available. Sediment trap data (at 853 and 3,931 m depth, stars in Figure 1) from a location close to our eastern cores when compared to surface sediments records confirm that the fossil record in this region reflects the surface water conditions, despite the fact that 98% of the diatom production is dissolved at the sediment/water interface (Treppke et al., 1996). The species related to the summer upwelling and the weakly silicified taxa are not preserved. However, the remaining diatom assemblage hold other species found in the water column during the spring, autumn and winter seasons. Therefore, the authors consider that the diatom assemblage of surface sediments reflects the overlying surface-water hydrography. Similarly, diatom species found in the Congo River deep-sea fan surface sediments, in the eastern equatorial Atlantic, are related to the overlying water masses properties (Van Iperen et al., 1987). Despite fossil diatom assemblages reflect the diatom of overlying waters, the more robust taxa preferentially accumulate in sediment traps and in surface sediments (Treppke et al., 1996) and the presence of neritic species in the deep sediment trap suggests potential effects of transport from nearshore waters and or downslope transport or resuspension of sediments (Treppke et al., 1996).

The most abundant diatom species identified in our samples (*T. nitzschioides* and *T. oestrupii* principally) are generally heavily silicified and resistant to dissolution, consistent with the observation of preferential dissolution of fragile species in the water column (Treppke et al., 1996). The most abundant species after *T. nitzschioides* and *T. oestrupii* shed more light on the conditions in the overlaying water column (Figure 4): in all eastern cores, the third most abundant species in this sub-region (*R. bergonii*, *F. doliolus* and *Chaetoceros* resting spores) would reflect a more intense upwelling (Treppke et al., 1996), while in the central cores, the lightly silicified *N. bicapitata* in V30-40 would reflect an oceanic upwelling event (Treppke et al., 1996). Therefore, the diatom assemblages corresponding to the highest diatom abundance are indicative of increased nutrient content of the water through upwelling, suggesting enhanced productivity. In this case, increased diatom abundance does not result solely from preservation. However, increased abundance of *E.rex* fragments, a diatom species thriving in oligotrophic waters, points to a specific distribution of nutrients in the water column (*cf.* Section 5.3.2).

5.3. The Main Two Steps of the Deglacial Process

5.3.1. Surficial Freshening ca. 18 ka Inferred From Coccolithophores

About 2–3 ka before the diatom productivity event, the ratio between the coccolithophore *G. oceanica* and *E. huxleyi* indicates a change in coccolithophore productivity conditions associated with a surface water freshening centered at 18 ka (Figure 2b).

The contribution of *G.oceanica* is indeed typically higher than the contribution of *E. huxleyi* between 15.8 and 23 ka (N.B.: almost no data-points for this interval in RC13-189 and RC24-07). A similar pattern is observed for the same

time interval in a nearby extended coccolithophore record from our studied area showing peaks in abundance of *G. oceanica* during marine isotopic 2 (Henriksson, 2000). *E. huxleyi* is the dominant species in the Atlantic at Present (Okada & McIntyre, 1979), hence it is expected to show a consistent background level of abundance. The warm water species *G. oceanica* is considered an indicator of high productivity pulses (Winter & Martin, 1990). An interplay between switching abundances of *G. oceanica* and *E. huxleyi* (when one is high the other is low) has been observed in records from the Indian and Pacific Ocean (Houghton & Guptha, 1991) and from the Cariaco basin (Mertens et al., 2009): at all sites, it is interpreted that *G. oceanica* is favored over *E. huxleyi* in high fertility equatorial waters when monsoonal influence is high, likely due to nutrients input through monsoonal wind and induced upwelling. The concomitant decreased contribution of *F. profunda*, a common species of the lower photic zone indicative of surface water oligotrophy, support better surficial productivity conditions (Molfino & McIntyre, 1990). This relationship between both species is clearly accentuated by 18 ka, when boreal solar insolation increase (Figure 2b) and characterizing the last glacial termination (Denton et al., 2010). McIntyre et al. (1989) already evidenced this link between insolation and the north African monsoon. Here, the surface water freshening can be considered as evidence for the presence of the ITCZ rain belt over the studied sites. At Present, the ITCZ has an average position north of the equator (Philander et al., 1996) and its southward migration is likely the response to increased cooling and ice cover on the North Atlantic (Broccoli et al., 2006; Chiang & Bitz, 2005), possibly reflecting the onset of Heinrich Stadial 1 (Hodell et al., 2017) in the equatorial Atlantic. This period is marked by major AMOC perturbations (McManus et al., 2004) due to ice and meltwater injections into the North Atlantic (Bond et al., 1992; Broecker et al., 1992).

5.3.2. Water Column Alterations Revealed by the Diatoms and the Coccolithophores ca. 15.5 ka

The surface freshening episode is followed about 2–3 ka later by a prominent diatom productivity event. Increased diatom productivity (including *E. rex*) and in other siliceous microfossils at all sites (except RC16-66) ca. 15.5 ka is the main characteristic of this deglacial record indeed. *E. rex* indicates in situ productivity. This is not a bloom-forming marine species. It is found in oligotrophic open ocean conditions and can be found deeper in the water column (up to 140 m), below the nutricline (Villareal, 1993). At the same time, a higher contribution of *F. profunda* is registered. Several studies also refer *F. profunda* as a typical low photic zone species from low-latitude regions, indicative of a deeper nutricline (Molfino & McIntyre, 1990; Okada & McIntyre, 1977) and mostly abundant between 10°N and 5°S (Baumann et al., 2004). Therefore, both *E. rex* and *F. profunda* indicate stratified oligotrophic surface waters and nutrients availability in the lower part of the euphotic zone. Furthermore, *E. rex* is also found at frontal zones related to tropical instability waves (TIW) and or/where enhanced run-off of Si-rich waters can be found (Abrantes, 2001; Kemp et al., 2006) in the equatorial Atlantic. As *E. rex* is weakly silicified (Villareal, 1993), it is mainly recycled in the water column and its preservation in the sediments is attributed to rapid sinking due to breakdown of the stratification caused principally by TIW. The TIW are an interface between warm and cold SST near the equator that propagates westward (Figure 1). Nowadays, their occurrence and intensification during the boreal summer is coincident with the strengthening of the southeasterly trade winds and the seasonal appearance of the equatorial cold tongue (Grodsky et al., 2005). Thus, it is possible that during the time intervals when *E. rex* is abundant (ca. 16-14 ka) the equatorial Atlantic area was under the influence of TIW that broke the stratification and facilitated *E. rex* fragments rapid transport to depth and avoiding its dissolution and recycling.

The opal burial would have therefore occurred after the ITCZ returned northward. However, our records reveal that the diatom maxima occur in different context, likely reflecting their latitudinal positioning and the influence of the African continent: in RC13-189, V22-182 and RC24-01 (northern cores), it is preceded by an eolian input evidenced by the phytoliths and the freshwater diatoms; in RC24-07 and RC24-12 (southern cores), a possible coastal influence (increase in *Chaetoceros* resting spores and even freshwater diatoms) preceded the diatom maximum in combination with an eolian input; and finally, in V30-40 (central core), the indicators of oceanic upwelling and eolian input are simultaneous.

Intensification of the southeasterly trade winds and the northward displacement of the ITCZ triggered the development of the equatorial Atlantic cold tongue, with the shoaling and cooling of the mixed layer (Hastenrath & Lamb, 1978). These conditions would also supply nutrients to the surface with upwelled water, which would account for the peak in the overall diatom abundance at that time.

5.3.3. How AMOC Perturbations Contributed to Opal Burial ca. 15.5 ka

The succession of oceanographic settings depicted first by the coccolithophore and then by the diatom records is similar to the present-day seasonal variability over the equatorial Atlantic and the ITCZ-cold tongue complex (Mitchell & Wallace, 1992). First, during boreal spring, the ITCZ is located close to the equator (southward

position during the deglacial onset) and associated with high SST (indicated by the increase in *G. oceanica*) and weak trades winds. Then, during the boreal summer, the ITCZ migrates northward when southeasterly winds intensify. This results in the shoaling of the thermocline, with enhanced upwelling and vertical mixing (processes favoring nutrient availability in the euphotic zone, accompanied by increased diatom production), and eventually to the development of the Atlantic cold tongue (rapid sinking and preservation of *E.rex*). The SSW is believed to be a source of nutrients (Brzezinski et al., 2002; Matsumoto et al., 2002) at intermediate depth below the thermocline from which *E. rex* would have benefited. Internal wave breaking would also bring the nutrients associated with the SSW to the surface where they are used by the primary producers (Thiagarajan et al., 2014). The siliceous record in the equatorial Atlantic therefore may reflect large-scale changes in oceanic circulation during the last deglaciation that were likely initiated by the intensification of the easterly trade winds. Eventually, global circulation changes involving deep water changes associated with the SSW mass likely contributed to the exceptional diatom production and preservation in the sediments.

6. Conclusions

The microfossil analyses presented here refine the previous interpretation of climate-induced biogeochemical changes in the equatorial Atlantic and provide evidence of two main steps in the deglacial process. We show that multiple processes are required to explain the opal record during the deglaciation, and specifically identify contributions from eolian input as well as pelagic and coastal upwelling. The microfossil group/species abundance and assemblages help identify temporal and spatial changes in primary productivity conditions. A deglacial peak in the abundance of the deep-dwelling diatom *E. rex* and the coccolithophore *F. profunda* indicates increased nutrient-availability in the lower photic zone, possibly as a result of interactions with AAIW. The preservation of easily dissolved *E. rex* fragments in the sediments suggests the breakdown of water column stratification and rapid settling. Such conditions likely resulted from the formation of a cold tongue of upwelled waters triggered by the intensification of southerly winds and the development of TIW. The contribution of nutrient-rich southern-sourced water may have also occurred through mixing possibly related to internal wave breaking, and consequently contributed to the unusual production and preservation of diatoms during this important deglacial interval.

Additionally, the coccolithophore record reveals a productivity event associated with surficial freshening centered ca. 18 ka, possibly associated with increased boreal insolation.

Data Availability Statement

The microfossil data used for this research is available with open access at PANGAEA®—Data Publisher for Earth & Environmental Science via Gil et al. (2023) with license Creative Commons Attribution 4.0 International.

Acknowledgments
Research supported by Fundação para a Ciência e Tecnologia—FCT through projects MONA (PTDC/AAC-AMB/108449/2008), PEst-C/MAR/LA0015/2011, UIDB/04326/2020, UIDP/04326/2020, LA/P/0101/2020, and a postdoctoral fellowship (SFRH/BPD/87718/2012) to IMG; and the European Regional Development Fund (ERDF) through the COMPETE - Operational Competitiveness Program. The contribution of JFM was supported in part by the US-NSF. Thanks to L. Bradtmiller and the Lamont-Doherty Earth Observatory (Columbia University, New-York, USA) for providing the samples, Ana Alberto for technical support and Adina Paytan for reviewing an early draft of the manuscript. We finally thank the reviewers for their constructive comments.

References

Abrantes, F. (2001). Assessing the *Ethmodiscus* ooze problem: New perspective from a study of an eastern equatorial Atlantic core. *Deep Sea Research Part I: Oceanographic Research Papers*, *48*(1), 125–135. https://doi.org/10.1016/s0967-0637(00)00041-8

Abrantes, F., & Gil, I. M. (2013). Marine diatoms. In S. A. Elias (Ed.), *The encyclopedia of quaternary science* (pp. 816–824). Elsevier.

Abrantes, F., Gil, I. M., Lopes, C., & Castro, M. (2005). Quantitative diatom analyses-a faster cleaning procedure. *Deep-Sea Research I*, *52*(1), 189–198. https://doi.org/10.1016/j.dsr.2004.05.012

Ahn, J., & Brook, E. J. (2008). Atmospheric CO_2 and climate on millennial time scales during the last glacial period. *Science*, *322*(5898), 83–85. https://doi.org/10.1126/science.1160832

Anderson, R., Ali, S., Bradtmiller, L., Nielsen, S., Fleisher, M., Anderson, B., & Burckle, L. (2009). Wind-driven upwelling in the Southern Ocean and the deglacial rise in atmospheric CO_2. *Science*, *323*(5920), 1443–1448. https://doi.org/10.1126/science.1167441

Arellano-Torres, E., Pichevin, L. E., & Ganeshram, R. S. (2011). High-resolution opal records from the eastern tropical Pacific provide evidence for silicic acid leakage from HNLC regions during glacial periods. *Quaternary Science Reviews*, *30*(9–10), 1112–1121. https://doi.org/10.1016/j.quascirev.2011.02.002

Armbrust, E. V. (2009). The life of diatoms in the world's oceans. *Nature*, *459*(7244), 185–192. https://doi.org/10.1038/nature08057

Batterbee, R. (1973). A new method for estimating absolute microfossil numbers with special reference to diatoms. *Limnology & Oceanography*, *18*(4), 647–653. https://doi.org/10.4319/lo.1973.18.4.0647

Baumann, K.-H., Böckel, B., & Frenz, M. (2004). Coccolith contribution to South Atlantic carbonate sedimentation. In H. R. Thierstein & J. R. Young (Eds.), *Coccolithophores* (pp. 367–402). Springer.

Berger, A. (1992). *Orbital variations and insolation database*. IGBP PAGES/World Data Center-A for Paleoclimatology Data. Contribution Series# 92-007.

Bond, G., Heinrich, H., Broecker, W., Labeyrie, L., McManus, J., Andrews, J., et al. (1992). Evidence for massive discharges of icebergs into the North Atlantic Ocean during the last glacial period. *Nature*, *360*(6401), 245–249. https://doi.org/10.1038/360245a0

Bradtmiller, L., Anderson, R., Fleisher, M., & Burckle, L. (2006). Diatom productivity in the equatorial Pacific Ocean from the last glacial period to the present: A test of the silicic acid leakage hypothesis. *Paleoceanography*, *21*(4), PA4201. https://doi.org/10.1029/2006PA001282

Bradtmiller, L., Anderson, R., Fleisher, M., & Burckle, L. (2007). Opal burial in the equatorial Atlantic Ocean over the last 30 ka: Implications for glacial-interglacial changes in the ocean silicon cycle. *Paleoceanography*, *22*(4), PA4216. https://doi.org/10.1029/2007PA001443

Bradtmiller, L. I., McGee, D., Awalt, M., Evers, J., Yerxa, H., Kinsley, C. W., & de Menocal, P. B. (2016). Changes in biological productivity along the northwest African margin over the past 20,000 years. *Paleoceanography*, *31*(1), 185–202. https://doi.org/10.1002/2015pa002862

Bradtmiller, L. I., McManus, J. F., & Robinson, L. F. (2014). $^{231}Pa/^{230}Th$ evidence for a weakened but persistent Atlantic meridional overturning circulation during Heinrich Stadial 1. *Nature Communications*, *5*, 5817. https://doi.org/10.1038/ncomms6817

Broccoli, A. J., Dahl, K. A., & Stouffer, R. J. (2006). Response of the ITCZ to Northern Hemisphere cooling. *Geophysical Research Letters*, *33*(1). https://doi.org/10.1029/2005GL024546

Broecker, W., Bond, G., Klas, M., Clark, E., & McManus, J. (1992). Origin of the northern Atlantic's Heinrich events. *Climate Dynamics*, *6*(3–4), 265–273. https://doi.org/10.1007/bf00193540

Brzezinski, M. A., Pride, C. J., Franck, V. M., Sigman, D. M., Sarmiento, J. L., Matsumoto, K., et al. (2002). A switch from $Si(OH)_4$ to NO_3^- depletion in the glacial Southern Ocean. *Geophysical Research Letters*, *29*(12), 1564. https://doi.org/10.1029/2001GL014349

Chiang, J. C., & Bitz, C. M. (2005). Influence of high latitude ice cover on the marine Intertropical Convergence Zone. *Climate Dynamics*, *25*(5), 477–496. https://doi.org/10.1007/s00382-005-0040-5

Cléroux, C., de Menocal, P., Arbuszewski, J., & Linsley, B. (2013). Reconstructing the upper water column thermal structure in the Atlantic Ocean. *Paleoceanography*, *28*(3), 503–516. https://doi.org/10.1002/palo.20050

CLIMAP. (1976). The surface of the ice-age Earth. *Science*, *191*(4232), 1131–1137. https://doi.org/10.1126/science.191.4232.1131

Conley, D. J., Kilham, S. S., & Theriot, E. (1989). Differences in silica content between marine and freshwater diatoms. *Limnology & Oceanography*, *34*(1), 205–212. https://doi.org/10.4319/lo.1989.34.1.0205

Costa, K. M., Jacobel, A. W., McManus, J. F., Anderson, R. F., Winckler, G., & Thiagarajan, N. (2017). Productivity patterns in the equatorial Pacific over the last 30,000 years. *Global Biogeochemical Cycles*, *31*(5), 850–865. https://doi.org/10.1002/2016gb005579

Denton, G. H., Anderson, R. F., Toggweiler, J., Edwards, R., Schaefer, J., & Putnam, A. (2010). The last glacial termination. *Science*, *328*(5986), 1652–1656. https://doi.org/10.1126/science.1184119

Dubois, N., Kienast, M., Kienast, S., Calvert, S. E., François, R., & Anderson, R. F. (2010). Sedimentary opal records in the eastern equatorial Pacific: It is not all about leakage. *Global Biogeochemical Cycles*, *24*(4). https://doi.org/10.1029/2010GB003821

Farmer, E. C., Kaplan, A., de Menocal, P. B., & Lynch-Stieglitz, J. (2007). Corroborating ecological depth preferences of planktonic foraminifera in the tropical Atlantic with the stable oxygen isotope ratios of core top specimens. *Paleoceanography*, *22*, PA3205. https://doi.org/10.1029/2006PA001361

Flores, J., & Sierro, F. (1997). Revised technique for calculation of calcareous nannofossil accumulation rates. *Micropaleontology*, *43*(3), 321–324. https://doi.org/10.2307/1485832

Folger, D., Burckle, L., & Heezen, B. (1967). Opal phytoliths in a North Atlantic dust fall. *Science*, *155*(3767), 1243–1244. https://doi.org/10.1126/science.155.3767.1243

Gil, I. M., Keigwin, L. D., & Abrantes, F. G. (2009). Deglacial diatom productivity and surface ocean properties over the Bermuda Rise, northeast Sargasso Sea. *Paleoceanography*, *24*(4), PA4101. https://doi.org/10.1029/2008PA001729

Gil, I. M., McManus, J. F., Rebotim, A., Narciso, A., Salgueiro, E., & Abrantes, F. (2023). Various siliceous micro-fossil and calcacerous nannofossil records from the Equatorial Atlantic (last 25 ka) [Dataset]. PANGAEA. https://doi.org/10.1594/PANGAEA.960036

Grodsky, S. A., Carton, J. A., & McClain, C. R. (2008). Variability of upwelling and chlorophyll in the equatorial Atlantic. *Geophysical Research Letters*, *35*(3), L03610. https://doi.org/10.1029/2007GL032466

Grodsky, S. A., Carton, J. A., Provost, C., Servain, J., Lorenzzetti, J. A., & McPhaden, M. J. (2005). Tropical instability waves at 0º N, 23º W in the Atlantic: A case study using Pilot Research Moored Array in the Tropical Atlantic (PIRATA) mooring data. *Journal of Geophysical Research*, *110*(C8), C08010. https://doi.org/10.1029/2005JC002941

Hastenrath, S., & Lamb, P. (1978). On the dynamics and climatology of surface flow over the equatorial oceans. *Tellus*, *30*(5), 436–448. https://doi.org/10.3402/tellusa.v30i5.10387

Hendry, K. R., Gong, X., Knorr, G., Pike, J., & Hall, I. R. (2016). Deglacial diatom production in the tropical North Atlantic driven by enhanced silicic acid supply. *Earth and Planetary Science Letters*, *438*, 122–129. https://doi.org/10.1016/j.epsl.2016.01.016

Henriksson, A. (2000). Coccolithophore response to oceanographic changes in the equatorial Atlantic during the last 200,000 years. *Palaeogeography, Palaeoclimatology, Palaeoecology*, *156*(1–2), 161–173. https://doi.org/10.1016/s0031-0182(99)00139-x

Higginson, M. J., & Altabet, M. A. (2004). Initial test of the silicic acid leakage hypothesis using sedimentary biomarkers. *Geophysical Research Letters*, *31*(18), L18303. https://doi.org/10.1029/2004GL020511

Hodell, D. A., Nicholl, J. A., Bontognali, T. R., Danino, S., Dorador, J., Dowdeswell, J. A., et al. (2017). Anatomy of Heinrich Layer 1 and its role in the last deglaciation. *Paleoceanography*, *32*(3), 284–303. https://doi.org/10.1002/2016pa003028

Houghton, S. D., & Guptha, M. S. (1991). Monsoonal and fertility controls on recent marginal sea and continental shelf coccolith assemblages from the western Pacific and northern Indian oceans. *Marine Geology*, *97*(3–4), 251–259. https://doi.org/10.1016/0025-3227(91)90119-o

Imbrie, J., & Kipp, N. G. (1971). A new micropaleontological method for quantitative paleoclimatology: Application to a late Pleistocene Caribbean core. In K. K. Turekian (Ed.), *Late Cenozoic glacial ages* (pp. 71–181). Yale Univ. Press.

Kemp, A., Pearce, R., Grigorov, I., Rance, J., Lange, C., Quilty, P., & Salter, I. (2006). Production of giant marine diatoms and their export at oceanic frontal zones: Implications for Si and C flux from stratified oceans. *Global Biogeochemical Cycles*, *20*(4). https://doi.org/10.1029/2006GB002698

Kolbe, R. (1957). Fresh-water diatoms from Atlantic deep-sea sediments. *Science*, *126*(3282), 1053–1056. https://doi.org/10.1126/science.126.3282.1053

Lange, C. B., Treppke, U. F., & Fischer, G. (1994). Seasonal diatom fluxes in the Guinea Basin and their relationships to trade winds, hydrography and upwelling events. *Deep Sea Research Part I: Oceanographic Research Papers*, *41*(5–6), 859865–863878. https://doi.org/10.1016/0967-0637(94)90080-9

Levitus, S., Locarnini, R. A., Boyer, T. P., Mishonov, A. V., Antonov, J. I., Garcia, H. E., et al. (2002). World Ocean Atlas 2009.

Locarnini, R. A., Mishonov, A. V., Baranova, O. K., Boyer, T. P., Zweng, M. M., Garcia, H. E., et al. (2019). World Ocean Atlas 2018. In *NOAA Atlas NESDIS 81 Volume 1: Temperature* (p. 52).

Maldonado, M., López-Acosta, M., Sitjà, C., García-Puig, M., Galobart, C., Ercilla, G., & Leynaert, A. (2019). Sponge skeletons as an important sink of silicon in the global oceans. *Nature Geoscience*, *12*(10), 815–822. https://doi.org/10.1038/s41561-019-0430-7

Matsumoto, K., & Sarmiento, J. L. (2008). A corollary to the silicic acid leakage hypothesis. *Paleoceanography*, *23*(2). https://doi.org/10.1029/2007PA001515

Matsumoto, K., Sarmiento, J. L., & Brzezinski, M. A. (2002). Silicic acid leakage from the Southern Ocean: A possible explanation for glacial atmospheric pCO_2. *Global Biogeochemical Cycles*, *16*(3), 5-1–5-23. https://doi.org/10.1029/2001GB001442

Maynard, N. G. (1976). Relationship between diatoms in surface sediments of the Atlantic Ocean and the biological and physical oceanography of overlying waters. *Paleobiology*, *2*, 99–121. https://doi.org/10.1017/s0094837300003390

McIntyre, A., Ruddiman, W. F., Karlin, K., & Mix, A. C. (1989). Surface water response of the equatorial Atlantic Ocean to orbital forcing. *Paleoceanography*, *4*(1), 19–55. https://doi.org/10.1029/pa004i001p00019

McManus, J. F., Francois, R., Gherardi, J.-M., Keigwin, L. D., & Brown-Leger, S. (2004). Collapse and rapid resumption of Atlantic meridional circulation linked to deglacial climate changes. *Nature*, *428*(6985), 834–837. https://doi.org/10.1038/nature02494

Meckler, A., Sigman, D., Gibson, K., François, R., Martínez-García, A., Jaccard, S., et al. (2013). Deglacial pulses of deep-ocean silicate into the subtropical North Atlantic Ocean. *Nature*, *495*(7442), 495–498. https://doi.org/10.1038/nature12006

Mertens, K. N. J. M., Lynn, M., Aycard, M., Lin, H.-L., & Louwye, S. (2009). Coccolithophores as palaeoecological indicators for shifts of the ITCZ in the Cariaco Basin during the late Quaternary. *Journal of Quaternary Science*, *24*(2), 159–174. https://doi.org/10.1002/jqs.1194

Mitchell, T. P., & Wallace, J. M. (1992). The annual cycle in equatorial convection and sea surface temperature. *Journal of Climate*, *5*(10), 1140–1156. https://doi.org/10.1175/1520-0442(1992)005<1140:taciec>2.0.co;2

Mix, A. C., & Ruddiman, W. F. (1985). Structure and timing of the last deglaciation: Oxygen-isotope evidence. *Quaternary Science Reviews*, *4*(2), 59–108. https://doi.org/10.1016/0277-3791(85)90015-0

Molfino, B., & McIntyre, A. (1990). Nutricline variation in the equatorial Atlantic coincident with the Younger Dryas. *Paleoceanography*, *5*(6), 997–1008. https://doi.org/10.1029/pa005i006p00997

Mortlock, R. A., & Froelich, P. N. (1989). A simple method for the rapid determination of biogenic opal in pelagic marine sediments. Deep Sea Research Part A. *Oceanographic Research Papers*, *36*(9), 1415–1426. https://doi.org/10.1016/0198-0149(89)90092-7

Nelson, D. M., Tréguer, P., Brzezinski, M. A., Leynaert, A., & Quéguiner, B. (1995). Production and dissolution of biogenic silica in the ocean: Revised global estimates, comparison with regional data and relationship to biogenic sedimentation. *Global Biogeochemical Cycles*, *9*(3), 359–372. https://doi.org/10.1029/95gb01070

Okada, H., & McIntyre, A. (1977). Modern coccolithophores of the Pacific and North Atlantic oceans. *Micropaleontology*, *23*, 1–55. https://doi.org/10.2307/1485309

Okada, H., & McIntyre, A. (1979). Seasonal distribution of modern coccolithophores in the western North Atlantic Ocean. *Marine Biology*, *54*(4), 319–328. https://doi.org/10.1007/bf00395438

Parmenter, C., & Folger, D. (1974). Eolian biogenic detritus in deep sea sediments: A possible index of equatorial ice age aridity. *Science*, *185*(4152), 695–698. https://doi.org/10.1126/science.185.4152.695

Pérez, V., Fernández, E., Marañón, E., Serret, P., & García-Soto, C. (2005). Seasonal and interannual variability of chlorophyll a and primary production in the equatorial Atlantic: *In situ* and remote sensing observations. *Journal of Plankton Research*, *27*(2), 189–197. https://doi.org/10.1093/plankt/fbh159

Philander, S., Gu, D., Lambert, G., Li, T., Halpern, D., Lau, N., & Pacanowski, R. (1996). Why the ITCZ is mostly north of the equator. *Journal of Climate*, *9*(12), 2958–2972. https://doi.org/10.1175/1520-0442(1996)009<2958:wtiimn>2.0.co;2

Pichevin, L. E., Ganeshram, R. S., & Dumont, M. (2020). Deglacial Si remobilisation from the deep-ocean reveals biogeochemical and physical controls on glacial atmospheric CO_2 levels. *Earth and Planetary Science Letters*, *543*, 116332. https://doi.org/10.1016/j.epsl.2020.116332

Pitcher, G. (1990). Phytoplankton seed populations of the Cape Peninsula upwelling plume, with particular reference to resting spores of *Chaetoceros* (*Bacillariophyceae*) and their role in seeding upwelling waters. *Estuarine, Coastal and Shelf Science*, *31*(3), 283–301. https://doi.org/10.1016/0272-7714(90)90105-z

Poggemann, D.-W., Hathorne, E. C., Nürnberg, D., Frank, M., Bruhn, I., Reißig, S., & Bahr, A. (2017). Rapid deglacial injection of nutrients into the tropical Atlantic via Antarctic intermediate water. *Earth and Planetary Science Letters*, *463*, 118–126. https://doi.org/10.1016/j.epsl.2017.01.030

Pokras, E. M. (1991). Source areas and transport mechanisms for freshwater and brackish-water diatoms deposited in pelagic sediments of the equatorial Atlantic. *Quaternary Research*, *35*(1), 144–156. https://doi.org/10.1016/0033-5894(91)90101-a

Pokras, E. M., & Mix, A. C. (1985). Eolian evidence for spatial variability of late Quaternary climates in tropical Africa. *Quaternary Research*, *24*(2), 137–149. https://doi.org/10.1016/0033-5894(85)90001-8

Pokras, E. M., & Molfino, B. (1986). Oceanographic control of diatom abundances and species distributions in surface sediments of the tropical and southeast Atlantic. *Marine Micropaleontology*, *10*(1–3), 165–188. https://doi.org/10.1016/0377-8398(86)90028-9

Pokras, E. M., & Ruddiman, W. F. (1989). *Evolution of south Saharan/Sahelian aridity based on freshwater diatoms (genus Melosira)* and opal phytoliths: Sites 662 and 664 (pp. 143–148). Proc Ocean Drilling Program Sci Res.

Prospero, J. (1996). Saharan dust transport over the North Atlantic Ocean and Mediterranean: An overview. In S. Guerzoni & R. Chester (Eds.), *The impact of desert dust across the Mediterranean* (pp. 133–151). Kluwer Academic Publishers.

Prospero, J. M., Bonatti, E., Schubert, C., & Carlson, T. N. (1970). Dust in the Caribbean atmosphere traced to an African dust storm. *Earth and Planetary Science Letters*, *9*(3), 287–293. https://doi.org/10.1016/0012-821x(70)90039-7

Romero, O. E., Leduc, G., Vidal, L., & Fischer, G. (2011). Millennial variability and long-term changes of the diatom production in the eastern equatorial Pacific during the last glacial cycle. *Paleoceanography*, *26*(2). https://doi.org/10.1029/2010pa002099

Schlitzer, R. (2020). Ocean data view. https://odv.awi.de

Schrader, H., Swanberg, I., Burckle, L., & Grønlien, L. (1993). Diatoms in recent Atlantic (20°S to 70°N latitude) sediments: Abundance patterns and what they mean. *Hydrobiologia*, *269–743*, 129–135.

Schrader, H. J., & Gersonde, R. (1978). Diatoms and silicoflagellates. *Utrecht Micropaleontological Bulletins*, *17*, 129–176.

Shackleton, N. (1974). *Attainment of isotopic equilibrium between ocean water and the benthonic foraminifera genus Uvigerina*: Isotopic changes in the ocean during the last glacial, Les methodes quantitatives d'etude des variations du climax au cours du Pleistocene. Colloques Internationaux du Centre National de la Recherche Scientifique (CNRS).

Siegenthaler, U., Stocker, T. F., Monnin, E., Lüthi, D., Schwander, J., Stauffer, B., et al. (2005). Stable carbon cycle–climate relationship during the late Pleistocene. *Science*, *310*(5752), 1313–1317. https://doi.org/10.1126/science.1120130

Steph, S., Regenberg, M., Tiedemann, R., Mulitza, S., & Nürnberg, D. (2009). Stable isotopes of planktonic foraminifera from tropical Atlantic/Caribbean core-tops: Implications for reconstructing upper ocean stratification. *Marine Micropaleontology*, *71*(1–2), 1–19. https://doi.org/10.1016/j.marmicro.2008.12.004

Tegen, I., Heinold, B., Todd, M., Helmert, J., Washington, R., & Dubovik, O. (2006). Modelling soil dust aerosol in the Bodélé depression during the BoDEx campaign. *Atmospheric Chemistry and Physics*, *6*(12), 4345–4359. https://doi.org/10.5194/acp-6-4345-2006

Thiagarajan, N., & McManus, J. F. (2019). Productivity and sediment focusing in the Eastern Equatorial Pacific during the last 30,000 years. *Deep Sea Research Part I: Oceanographic Research Papers*, *147*, 100–110. https://doi.org/10.1016/j.dsr.2019.03.007

Thiagarajan, N., Subhas, A. V., Southon, J. R., Eiler, J. M., & Adkins, J. F. (2014). Abrupt pre-Bølling-Allerød warming and circulation changes in the deep ocean. *Nature*, *511*(7507), 75–78. https://doi.org/10.1038/nature13472

Treppke, U. F., Lange, C. B., & Wefer, G. (1996). Vertical fluxes of diatoms and silicoflagellates in the eastern equatorial Atlantic, and their contribution to the sedimentary record. *Marine Micropaleontology*, *28*(1), 73–96. https://doi.org/10.1016/0377-8398(95)00046-1

Van Iperen, J., Van Weering, T., Jansen, J., & Van Bennekom, A. (1987). Diatoms in surface sediments of the Zaire deep-sea fan (SE Atlantic Ocean) and their relation to overlying water masses. *Netherlands Journal of Sea Research*, *21*(3), 203–217. https://doi.org/10.1016/0077-7579(87)90013-5

Verardo, D. J., & McIntyre, A. (1994). Production and destruction: Control of biogenous sedimentation in the tropical Atlantic 0–300,000 years BP. *Paleoceanography*, *9*(1), 63–86. https://doi.org/10.1029/93pa02901

Villareal, T. A. (1993). Abundance of the giant diatom *Ethmodiscus* in the southwest Atlantic Ocean and central Pacific gyre. *Diatom Research*, *8*(1), 171–177. https://doi.org/10.1080/0269249x.1993.9705248

Waliser, D., & Jiang, X. (2015). Tropical meteorology and climate. In G. North, J. Pyle, & F. Zhang (Eds.), *Encyclopedia of atmospheric sciences* (2nd ed., pp. 121–131). Academic Press.

Washington, R., Todd, M., Middleton, N. J., & Goudie, A. S. (2003). Dust-storm source areas determined by the total ozone monitoring spectrometer and surface observations. *Annals of the Association of American Geographers*, *93*(2), 297–313. https://doi.org/10.1111/1467-8306.9302003

Winter, A., & Martin, K. (1990). Late Quaternary history of the Agulhas current. *Paleoceanography*, *5*(4), 479–486. https://doi.org/10.1029/pa005i004p00479